

Reprint, In Press, Corrected Proof,
Available online 1 May 2009

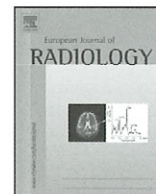
ISSN 0720-048X

European Journal of
RADIOLOGY

**A comparative evaluation of Cone Beam
Computed Tomography (CBCT) and
Multi-Slice CT (MSCT):
Part I. On subjective image quality**

Xin Liang, Reinhilde Jacobs, Bassam Hassan, Limin Li, Ruben Pauwels,
Livia Corpas, Paulo Couto Souza, Wendy Martens, Maryam Shahbazian,
Arie Alonso, Ivo Lambrichts

www.elsevier.com/locate/ejrad



A comparative evaluation of Cone Beam Computed Tomography (CBCT) and Multi-Slice CT (MSCT)

Part I. On subjective image quality

Xin Liang^{a,b,*}, Reinhilde Jacobs^a, Bassam Hassan^c, Limin Li^d, Ruben Pauwels^a, Livia Corpas^a, Paulo Couto Souza^a, Wendy Martens^e, Maryam Shahbazian^a, Arie Alonso^f, Ivo Lambrichts^e

^a Oral Imaging Centre, School of Dentistry, Oral Pathology and Maxillofacial Surgery, Faculty of Medicine, Catholic University of Leuven, Belgium

^b College of Stomatology, Dalian Medical University, China

^c Department of Oral Radiology, Academic Centre for Dentistry Amsterdam (ACTA), Amsterdam, The Netherlands

^d Department of Paediatric Dentistry and Special Dental Care, School of Dentistry, Oral Pathology and Maxillofacial Surgery, Faculty of Medicine, Catholic University of Leuven, Belgium

^e Department of Basic Medical Sciences, Faculty of Medicine, University of Hasselt, Diepenbeek, Belgium

^f Department of Biostatistics and Statistical Bioinformatics, Universiteit Hasselt, Belgium

ARTICLE INFO

Article history:

Received 29 January 2009

Accepted 24 March 2009

Keywords:

Cone Beam Computed Tomography

Dentomaxillofacial

Image quality

Mandible

Anatomical landmarks

ABSTRACT

Aims: To compare image quality and visibility of anatomical structures in the mandible between five Cone Beam Computed Tomography (CBCT) scanners and one Multi-Slice CT (MSCT) system.

Materials and methods: One dry mandible was scanned with five CBCT scanners (Accuitomo 3D, i-CAT, NewTom 3G, Galileos, Scanora 3D) and one MSCT system (Somatom Sensation 16) using 13 different scan protocols. Visibility of 11 anatomical structures and overall image noise were compared between CBCT and MSCT. Five independent observers reviewed the CBCT and the MSCT images in the three orthographic planes (axial, sagittal and coronal) and assessed image quality on a five-point scale.

Results: Significant differences were found in the visibility of the different anatomical structures and image noise level between MSCT and CBCT and among the five CBCT systems ($p=0.0001$). Delicate structures such as trabecular bone and periodontal ligament were significantly less visible and more variable among the systems in comparison with other anatomical structures ($p=0.0001$). Visibility of relatively large structures such as mandibular canal and mental foramen was satisfactory for all devices. The Accuitomo system was superior to MSCT and all other CBCT systems in depicting anatomical structures while MSCT was superior to all other CBCT systems in terms of reduced image noise.

Conclusions: CBCT image quality is comparable or even superior to MSCT even though some variability exists among the different CBCT systems in depicting delicate structures. Considering the low radiation dose and high-resolution imaging, CBCT could be beneficial for dentomaxillofacial radiology.

© 2009 Elsevier Ireland Ltd. All rights reserved.

1. Introduction

Digital two-dimensional (2D) intraoral and panoramic radiography have been widely adopted by dentists in the last decade

* Corresponding author at: Oral Imaging Centre, School of Dentistry, Oral Pathology and Maxillofacial Surgery, Faculty of Medicine, Catholic University of Leuven, Kapucijnenvoer 7, B-3000 Leuven, Belgium. Tel.: +32 16 332951; fax: +32 16 332951.

E-mail addresses: Xin.Liang@med.kuleuven.be (X. Liang), Reinhilde.Jacobs@uz.kuleuven.be (R. Jacobs), b.hassan@acta.nl (B. Hassan), Limin.Li@uz.kuleuven.be (L. Li), Ruben.Pauwels@med.kuleuven.be (R. Pauwels), LiviaCorpas@gmail.com (L. Corpas), Paulo.CoutoSouza@med.kuleuven.be (P.C. Souza), wendy.martens@uhasselt.be (W. Martens), Maryam.Shahbazian@student.kuleuven.be (M. Shahbazian), ariel.alonso@uhasselt.be (A. Alonso), Ivo.Lambrichts@uhasselt.be (I. Lambrichts).

0720-048X/\$ – see front matter © 2009 Elsevier Ireland Ltd. All rights reserved.
doi:10.1016/j.ejrad.2009.03.042

[1,2]. However, 2D radiographic images are difficult to interpret because of the overlapping of complex osseous structure. Anatomic structures such as the lingual foramen and incisive canal, which contain neuro-vascularisation can hardly be defined. Also, the lingual cortical bone of the mandible and width of the alveolar ridge cannot be accurately assessed [3–7]. The development of computed tomography (CT) enabled three-dimensional (3D) assessment of craniofacial structures. CT has become a widely available means for head and neck diagnosis [8,9] and various oral surgical procedures [10].

However, CT is still not ideal for the particular diagnostic task in dental applications, such as impacted teeth or apical lesions. Excessive radiation exposure, increased cost and limited availability impede the routine use of this technology for dental applications. Cone Beam CT (CBCT) offers a promising alternative approach

Table 1
Overview of the CT devices and the selected scan protocols.

CT device	Option	kV	mA	Scanning time (s)	FOV ^a (cm)	Pixel resolution (mm)	Slice thickness (mm)
Accuitomo 3D	0.5 mm ST ^b	80	4	17.5	4 × 3	0.125/0.125	0.5
	1 mm ST ^b			17.5	4 × 3	0.125/0.125	1
Scanora 3D	MSR ^c	85	10	20	10 × 7.5	0.3/0.3	0.3
	MHR ^d			20	10 × 7.5	0.2/0.2	0.2
	SHR ^e			20	6 × 6	0.15/0.15	0.15
NewTom 3G	h-HR ^f	110	3	36	10 × 10	0.18/0.18	0.1
	HR ^g			36	15 × 15	0.18/0.18	0.4
	SR ^h			36	20 × 20	0.4/0.4	0.6
i-CAT	Full	120	5.5	20	16 × 13	0.4/0.4	0.4
	MaxRes ⁱ			40	16 × 6	0.2/0.2	0.2
Galileos	HCM ^j	85	5	14	15 × 15	0.3/0.3	0.3
Somatom Sensation 16	H70h	120	90	20	25 × 9	0.28/0.28	0.3
	H60s	120	80	20	25 × 7.6	0.48/0.48	0.5

^a FOV: imaging field of view (diameter × height).

^b ST: slice thickness.

^c MSR: (Scanora) Medium field Standard Resolution.

^d MHR: (Scanora) Medium field High Resolution.

^e SHR: (Scanora) Small field High Resolution.

^f h-HR: (NewTom) very High Resolution.

^g HR: (NewTom) High Resolution.

^h SR: (NewTom) Standard Resolution.

ⁱ MaxRes: (iCT) Maximum Resolution.

^j HCM: (Galileos) High Contrast Mode.

since it provides sub-millimetre resolution images of high diagnostic quality, with short scanning time and reduced radiation dose up to 15 times lower than Multi-Slice CT scans (MSCT) [11]. CBCT has been used for several important oral and maxillofacial surgery applications including implant placement [12–16], bone and tooth fractures [17,18], temporomandibular joint examination [19], orthodontic cases (cleft, tooth impaction, and position of osteosynthetic screws) [20], third molar removal [21] and endodontic cases (root canal evaluation, apical lesions and root resorption) [22,23]. All former reports revealed sufficient image quality and information acquired with CBCT devices for different anatomical structures.

Previous studies comparing MSCT and CBCT demonstrated considerable variability in image quality expressed through different capability to depict anatomical structures in the maxillofacial region [24]. Most previous reports on CBCT image quality were limited, however, to only one or few systems [25–27]. In the meanwhile, various CBCT machines have been introduced or upgraded, making a standardized comparison of various CBCT machines contrasted to a MSCT machine mandatory. The aim of this study is to compare the subjective image quality and visibility of anatomical structures in the mandible between five CBCT and one MSCT scanners.

2. Materials and methods

One dry human mandible was obtained with approval from Institute for Biomedical Research (BIOMED of University Hasselt, Belgium). The mandible was placed in a plastic container and immersed in water to simulate soft-tissue [28] and then scanned with five Cone Beam CT scanners: NewTom 3G[®] (Quantitative Radiology, Verona, Italy), Accuitomo[®] 3D (Morita, Kyoto, Japan), i-CAT[®] (Imaging Sciences International, Hatfield, Pennsylvania, USA) and Galileos[®] (Sirona, Bensheim, Germany), Scanora[®] 3D (Soredex, Tuusula, Finland) and one MSCT-scanner Somatom Sensation[®] (Siemens, Erlangen, Germany).

Thirteen scans protocols with different field of views (FOVs) were selected for the six devices. Machine specification and scan-

ning protocol for each scanner are shown in Table 1. All scans were exported in DICOM 3 file format. Eleven anatomical structures were included in the analysis (Table 2). A five-point rating scale (1 = excellent, 2 = good, 3 = acceptable, 4 = poor, 5 = very poor) was used to assess the visibility of the 11 anatomic structures and overall image noise. Five observers assessed all images twice independently in different sessions with at least one week separation between the two sessions. The observers were all dentists who followed an advanced master programme in dental radiology. All observers were calibrated by training them in the software tool used in this study prior to conducting the observations. Observers were blinded to the type of CT machine and the selected scan protocol.

Two experiments were conducted:

Experiment 1: The 13 DICOM datasets from the six systems were imported in VolView visualization software (v.2.0, Kitware Inc., Clifton Park, New York) on a 19" flat panel screen (1280 × 1024, Philips Brilliance 200WP, Brussels, Belgium). The observers were asked to identify the anatomical structures and evaluate image noise by going through the dataset on three orthographic tomographic reconstructions (axial, frontal and sagittal). Observers

Table 2

General linear mixed models (GLMs) estimates of the visibility of anatomical structures on the six CT machines in experiments (1 and 2) on axial slices.

Anatomical structure	Estimate [*]	p value
Mental foramen	-0.1027	0.8218
Mandibular canal	-0.3482	0.4447
Cortical bone	-0.6598	0.1482
Pulp	-0.7941	0.1686
Dentin	-1.5715	0.9513
Incisive canal	-1.7078	0.4625
Enamel	-1.8258	0.1291
Lingual canal	-1.9394	0.3614
Periodontal ligament	-2.5574	0.0001
Trabecular bone	-2.7193	0.0001
Lamina dura	-4.04	0.0001

^{*} The higher the estimate, the better is the visibility of the anatomical structure. Notice that trabecular bone, periodontal ligament and lamina dura structures were less visible and statistically different ($p < 0.0001$) from other structures.

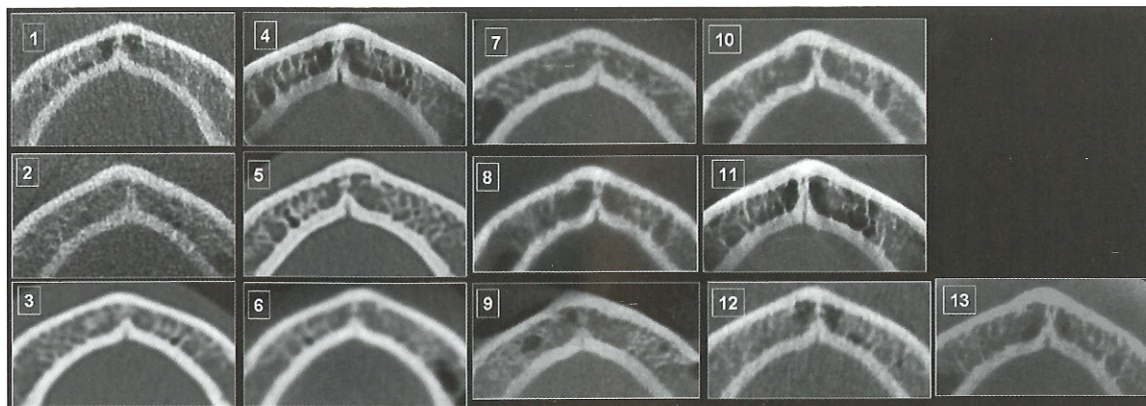


Fig. 1. One of the axis slice selections was standardized based on lingual canal identification showing identical lingual canal, cortical and trabecular bone in corresponding locations for the different scanners (1 = NewTom 3G very High Resolution; 2 = Galileos High Contrast Mode; 3 = Somatom Sensation 16 H60s; 4 = Accuitomo 3D/1 mm thickness; 5 = Somatom Sensation 16 H70h; 6 = i-CAT Full view; 7 = i-CAT Maximum Resolution; 8 = Scanora 3D Medium field Standard Resolution; 9 = NewTom 3G High Resolution; 10 = Scanora 3D Medium field High Resolution; 11 = Accuitomo 3D/0.5 mm thickness; 12 = NewTom 3G Standard Resolution; 13 = Scanora 3D Small field High Resolution).

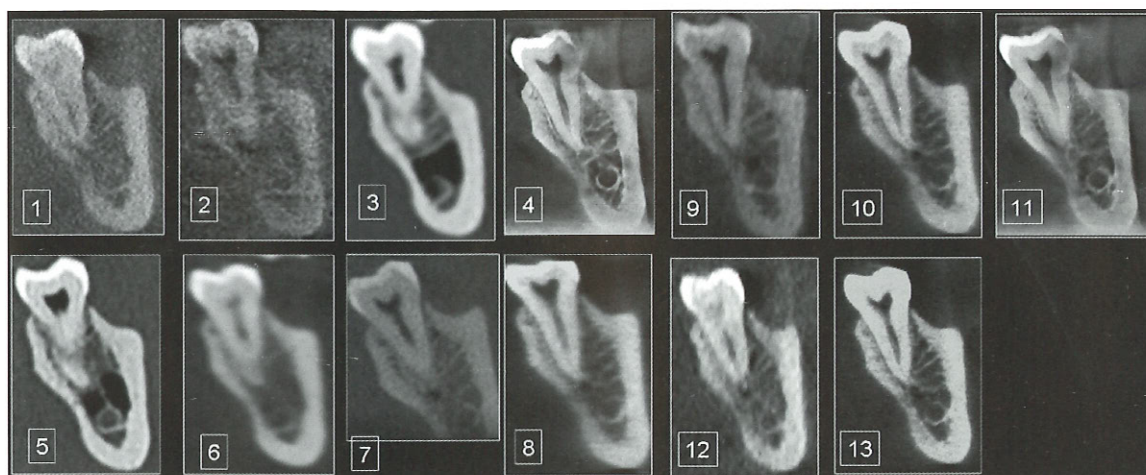


Fig. 2. One of the sagittal slice selections on mandibular canal identification showing the better image quality of mandibular canal, but less visible on enamel, trabecular bone, periodontal ligament space and lamina dura structures. Image No. 4 and No. 11 showed superior image quality in comparison with other images. These are two images from Accuitomo 3D.

were allowed to adjust the brightness and contrast settings for best display. This observation design was selected to mimic the routine diagnostic approach in which clinicians are permitted to adjust image display settings.

Experiment 2: One investigator who did not participate in making the measurements selected 13 images of each anatomical structure (one for each scan protocol) in each reconstruction plane (axial, frontal and sagittal). A total of 429 slices were selected (11 anatomical structures \times 13 FOV selections \times 3 reconstruction planes). Slice selection was standardized based on anatomical landmark identification depicting identical anatomical structures in corresponding locations for the different scanners (Figs. 1 and 2). To standardize viewing conditions, image brightness and contrast were calibrated by a light meter (PeakTech[®] 5025, Dürr Dental, Germany). Observers were not allowed to adjust the brightness and contrast settings or the reconstruction views to ensure a standardized comparison.

Statistical analysis

Inter- and intra-observers' agreements were quantified by weighted Kappa statistics using MedCalc (MedCalc[®] Version 9.3.9.0, Mariakerke, Belgium). Generalized linear mixed models (GLMs) (PROC NL MIXED, SAS[®] Institute Inc., Cary, New Caledo-

nia) were applied to analyse (1) overall variation in the visibility of anatomical structures (per structure) among the six CT systems, (2) variation in overall image quality (including all anatomical structures) among the six systems, (3) influence of image slice orientation (axial, sagittal or coronal) and (4) inter- and intra-observer variability. Kruskal–Wallis test was used to assess significant dif-

Table 3

General linear mixed models (GLMs) estimates of the capability of the six CT machines in visualizing anatomical structures on axial slices. The higher the estimate, the better is the overall capability of the system to visualize anatomical structures.

CT system	Estimate	p value
Accuitomo 3D 1 mm ST	3.5606	0.0001
Accuitomo 3D 0.5 mm ST	2.6436	0.0001
Somatom Sensation 16 H70h	1.5866	0.0001
i-CAT MaxRes	0.77	0.0161
NewTom 3G HR	0.367	0.2469
Scanora 3D MH	0.2901	0.37
Somatom Sensation H60s	0.2405	0.4467
Scanora 3D SH	0.1363	0.0001
i-CAT full	-0.3215	0.3043
Scanora 3D MSR	-0.8898	0.0052
NewTom 3G H-HR	-1.0106	0.0015
NewTom 3G SR	-1.7451	0.0001
Galileos HCM	-2.9497	0.0001

Table 4

Kruskal–Wallis test results ranking the different CT devices by their ability to visualize the trabecular bone, periodontal ligament and lamina dura. PN is the number of significant *p* value.

Anatomical structure				Image noise			
Trabecular bone	PN*	Periodontal ligament	PN	Lamina dura	PN	Noise level	PN
Accuitomo 3D 0.5 mm ST	5	Accuitomo 3D 1 mm ST	6	Accuitomo 3D 1 mm ST	7	Somatom Sensation 16 H70h	8
Accuitomo 3D 1 mm ST	5	Accuitomo 3D 0.5 mm ST	5	Accuitomo 3D 0.5 mm ST	5	Somatom Sensation H60s	0
Somatom Sensation 16 H70h	3	Somatom Sensation 16 H70h	5	Somatom Sensation 16 H70h	4	Accuitomo 3D 1 mm ST	0
i-CAT MaxRes	3	Scanora 3D SH	5	Scanora 3D MH	4	i-CAT full	0
NewTom 3G HR	3	NewTom 3G HR	2	Scanora 3D SH	3	i-CAT MaxRes	0
Scanora 3D MH	3	i-CAT MaxRes	0	NewTom 3G HR	-1	NewTom 3G SR	-1
Scanora 3D SH	3	Scanora 3D MH	0	i-CAT MaxRes	-1	Galileos HCM	-1
Scanora 3D MSR	1	Scanora 3D MSR	-1	Scanora 3D MSR	-1	Scanora 3D MSR	-1
Somatom Sensation H60s	-2	NewTom 3G h-HR	-4	i-CAT full	-2	NewTom 3G HR	-1
i-CAT full	-2	Somatom Sensation H60s	-4	NewTom 3G SR	-4	Scanora 3D MH	-1
NewTom 3G h-HR	-7	NewTom 3G SR	-4	NewTom 3G h-HR	-5	Accuitomo 3D 0.5 mm ST	-1
Galileos HCM	-7	Galileos HCM	-5	Galileos HCM	-5	NewTom 3G h-HR	-1
NewTom 3G SR	-8	i-CAT full	-5	Somatom Sensation H60s	-5	Scanora 3D SH	-1

PN* presents the number of significantly different CT devices from each other. Positive number means this CT device had significantly better image quality than the (PN) number of others (e.g. trabecular bone, Accuitomo 0.5 mm ST, PN = 5 means that the Accuitomo 0.5 mm ST scan had significantly better visibility of the trabecular bone than other five CT devices or settings). Negative number means the CT device was significantly worse on image quality than the number of others.

ferences among the six systems for depicting identical anatomical landmarks.

3. Results

Inter- and intra-observer agreement using weighted Kappa statistics was moderate for both experiment 1 and experiment 2 ($k = 0.48$ and 0.51), respectively. There was no significant difference in the measurements results between experiment 1 and experiment 2. GLMs estimates results for overall image quality of the six systems and visibility of the different anatomical structures are summarized in Tables 2 and 3. The trabecular bone, periodontal ligament and lamina dura were significantly less visible in comparison with other structures ($p = 0.0001$). Visibility of other anatomical structures was not significantly different (Table 3). There was no statistically significant influence of slice orientation on the visibility of landmarks among the six systems ($p = 0.6931$).

When ranking the visibility of trabecular bone, periodontal ligament and lamina dura per system and scan protocol, the Accuitomo system yielded the best results (Table 4 and Fig. 2). The MSCT was second to the Accuitomo in visualizing those structures. However, MSCT was superior to all CBCT system in terms of image noise (Table 4).

4. Discussion

Several scanning and reconstruction settings directly influence image quality of the acquired image, which in turn affects the radiographic visibility of anatomical structures and image noise level. Results from previous studies comparing two CBCT systems or one CBCT and one MSCT showed that CBCT image quality was comparable to that of MSCT [24]. The purpose of the present study was to compare the subjective image quality and hard tissue anatomic structures visibility of five CBCT systems with one MSCT system using different scanning FOV settings and reconstruction orientations (axial, coronal and sagittal).

The results of this study show that the image quality of five CBCT systems is comparable to that of MSCT and in one system (Accuitomo 3D), image quality was actually superior. This is clinically significant since CBCT delivers reduced dose to the patient in comparison with MSCT and it is also less expensive and widely available. These results, however, are only limited to hard tissue structures.

Because of the difference in design and clinical indication, all CT systems should not be treated equally and not one machine can be scored as optimal for all diagnostic procedures. However, the

results from both experiments show that all systems could visualize the mental foramen, mandibular canal, cortical bone, incisive canal and pulp space clearly irrespective to the scan or reconstruction setting. For lingual canal a high-resolution setting was needed to improve visibility with all machines.

The enamel and the dentine were moderately influenced by scanner type and the FOV settings. The trabecular bone, periodontal ligament space and lamina dura are relatively small and were the least visible anatomical structures with all machines and with all FOVs selections. Small FOV Accuitomo 3D and MSCT were superior to other systems in showing those structures. This corroborates previous findings [24,26]. In general, it could be stated that small FOV and high-resolution scans are optimal for detailed diagnostic tasks (e.g. endodontics), while large volume scans will be able delivering better 3D models. In that respect, it should be said that spiral CT remains superior for segmentation accuracy [24].

FOV selection is specific to each system. In several systems, the scanning volume can be adapted according to the clinical demands (e.g. Scanora, NewTom 3G and i-CAT). In others, only a single FOV selection is present (e.g. Galileos). FOV selection determines the size of the voxel used, which can be defined by the pixel resolution in the 'xy' plane and slice thickness in the 'z' plane. Image voxel size, which is highly correlated with spatial resolution, plays important role in the resulting quality of the image. Accuitomo 3D, for instance, had a very small voxel size (0.125 mm).

It is noteworthy, however, that spatial resolution is also highly correlated with image noise and contrast to noise ratio. The NewTom 3G high-resolution (NewTom h-HR) reconstruction, for example, had a nominal slice thickness of 0.1 mm and it had also a significantly higher level of noise in comparison with the standard reconstruction (NewTom SR). As such, a small FOV selection with a thin slice setting does not necessarily directly translate to better image quality or higher spatial resolution because the noise level can also be substantially increased. Although image noise in CBCT was higher than with MSCT, the influence of image noise from all CBCT systems was deemed 'tolerable', which correlates with earlier findings by Mozzo et al. [29].

5. Conclusions

The image quality of the CBCT systems included in this study was largely comparable to that of MSCT at different scan and reconstruction settings. Coupled with low radiation dose and short scanning time, CBCT system can play a vital role in the diagnosis of hard tissue structures of the dentomaxillofacial region.

References

- [1] Wenzel A. Digital radiography and caries diagnosis. *Dentomaxillofac Radiol* 1998;27:3–11.
- [2] Tal H, Moses O. A comparison of panoramic radiography with computed tomography in the planning of implant surgery. *Dentomaxillofac Radiol* 1991;20:40–2.
- [3] Tammisalo E, Hallikainen D, Kanerva H, Tammisalo T. Comprehensive oral X-ray diagnosis: Scanora multimodal radiography. A preliminary description. *Dentomaxillofac Radiol* 1992;21:9–15.
- [4] Jacobs R, Mraiwa N, van Steenberghe D, Gijbels F, Quirynen M. Appearance, location, course, and morphology of the mandibular incisive canal: an assessment on spiral CT scan. *Dentomaxillofac Radiol* 2002;31:322–7.
- [5] Liang X, Jacobs R, Lambrechts I. Appearance, location, course and morphology of the superior and inferior genial spinal foramina and their bony canals: an assessment on spiral CT scan. *Surg Radiol Anat* 2006;28:98–104.
- [6] Pohlentz P, Blessmann M, Blake F, Gbara A, Schmelzle R, Heiland M. Major mandibular surgical procedures as an indication for intraoperative imaging. *J Oral Maxillofac Surg* 2008;66:324–9.
- [7] Quirynen M, Lamoral Y, Dekeyser C, et al. CT scan standard reconstruction technique for reliable jaw bone volume determination. *Int J Oral Maxillofac Implants* 1990;5:384–9.
- [8] Fuchs T, Kachelriess M, Kalender WA. Technical advances in multi-slice spiral CT. *Rev Eur J Radiol* 2000;36:69–73.
- [9] Bou Serhal C, Jacobs R, Flygare L, Quirynen M, van Steenberghe D. Perioperative validation of localisation of the mental foramen. *Dentomaxillofac Radiol* 2002;31:39–43.
- [10] Sarment DP, Sukovic P, Clinthorne N. Accuracy of implant placement with a stereolithographic surgical guide. *Int J Oral Maxillofac Implants* 2003;18:571–7.
- [11] Scarfe WC, Farman AG, Sukovic P. Clinical applications of cone-beam computed tomography in dental practice. *J Can Dent Assoc* 2006;72:75–80.
- [12] Hatcher DC, Dial C, Mayorga C. Cone beam CT for pre-surgical assessment of implant sites. *J Calif Dent Assoc* 2003;31:825–33.
- [13] Madrigal C, Ortega R, Meniz C, López-Quiles J. Study of available bone for interforaminal implant treatment using cone-beam computed tomography. *Med Oral Pathol Oral Cir Bucal* 2008;13:E307–312.
- [14] Ito K, Gomi Y, Sato S, Arai Y, Shinoda K. Clinical application of a new compact CT system to assess 3-D images for the preoperative treatment planning of implants in the posterior mandible A case report. *Clin Oral Implants Res* 2001;12:539–42.
- [15] Chan Y, Siewerdsen JH, Rafferty MA, Moseley DJ, Jaffray DA, Irish JC. Cone-beam computed tomography on a mobile C-arm: novel intraoperative imaging technology for guidance of head and neck surgery. *J Otolaryngol Head Neck Surg* 2008;37:81–90.
- [16] Van Assche N, van Steenberghe D, Guerrero ME, et al. Accuracy of implant placement based on pre-surgical planning of three-dimensional cone-beam images: a pilot study. *J Clin Periodontol* 2007;34:816–21.
- [17] Heiland M, Schulze D, Rother U, Schmelzle R. Postoperative imaging of zygomaticomaxillary complex fractures using digital volume tomography. *J Oral Maxillofac Surg* 2004;62:1387–91.
- [18] Mol A, Tyndall DA, Rivera EM. In vitro assessment of local computed tomography for the detection of longitudinal tooth fractures. *Oral Surg Oral Med Oral Pathol Oral Radiol Endod* 2007;103:825–9.
- [19] Tsiklakis K, Syriopoulos K, Stamatakis HC. Radiographic examination of the temporomandibular joint using cone beam computed tomography. *Dentomaxillofac Radiol* 2004;33:196–201.
- [20] Korbmacher H, Kahl-Nieke B, Schöllchen M, Heiland M. Value of two cone-beam computed tomography systems from an orthodontic point of view. *J Orofac Orthop* 2007;68:278–89.
- [21] Nakagawa Y, Kobayashi K, Ishii H, et al. Preoperative application of limited cone beam computerized tomography as an assessment tool before minor oral surgery. *Int J Oral Maxillofac Surg* 2002;31:322–6.
- [22] Matherne RP, Angelopoulos C, Kuliild JC, Tira D. Use of cone-beam computed tomography to identify root canal systems in vitro. *J Endod* 2008;34:87–9.
- [23] Patel S, Dawood A, Ford TP, Whaites E. The potential applications of cone beam computed tomography in the management of endodontic problems. *Int Endod J* 2007;40:818–30.
- [24] Loubele M, Guerrero ME, Jacobs R, Suetens P, van Steenberghe D. A comparison of jaw dimensional and quality assessments of bone characteristics with cone-beam CT, spiral tomography, and multi-slice spiral CT. *Int J Oral Maxillofac Implants* 2007;22:446–54.
- [25] Guerrero ME, Jacobs R, Loubele M, Schutyser F, Suetens P, van Steenberghe D. State-of-the-art on cone beam CT imaging for preoperative planning of implant placement. *Clin Oral Invest* 2006;10:1–7.
- [26] Hashimoto K, Kawashima S, Kameoka S, et al. Comparison of image validity between cone beam computed tomography for dental use and multidetector row helical computed tomography. *Dentomaxillofac Radiol* 2007;36:465–71.
- [27] Schulze D, Heiland M, Blake F, Rother U, Schmelzle R. Evaluation of quality of reformatted images from two cone-beam computed tomographic systems. *J Craniomaxillofac Surg* 2005;33:19–23.
- [28] Suomalainen A, Vehmas T, Kortensniemi M, Robinson S, Peltola J. Accuracy of linear measurements using dental cone beam and conventional multislice computed tomography. *Dentomaxillofac Radiol* 2008;37:10–7.
- [29] Mozzo P, Procacci C, Tacconi A, Martini PT, Andreis IA. A new volumetric CT machine for dental imaging based on the cone-beam technique: preliminary results. *Eur Radiol* 1998;8:1558–64.